JSEE Vol. 25, No. 3&4, 2023 DOI: 10.48303/jsee.2023.2000949.1059

Research Paper

Performance Evaluation of Natural Gas Transmission Pipelines in Landslides

Soheil Hemmati[1], Akbar Vasseghi[2*] and Ebrahim Haghshenas[3]

1. Ph.D. Student, Structural Engineering Research Center, International Institute of Earthquake Engineering and Seismology (IIEES), Tehran, Iran
2. Associate Professor, Structural Engineering Research Center, International Institute of Earthquake Engineering and Seismology (IIEES), Tehran, Iran,
*Corresponding Author; email: vasseghi@iiees.ac.ir
3. Associate Professor, Geotechnical Engineering Research Center, International Institute of Earthquake Engineering and Seismology (IIEES), Tehran, Iran

Received: 26/04/2023
Revised: 02/09/2023
Accepted: 02/10/2023

ABSTRACT

The study aimed to evaluate the behavior of typical natural gas transmission pipelines in landslides and investigate the effect of various parameters such as internal pressure, pipe diameter, and soil type on their active lengths. Nonlinear Finite Element Analyses (FEA) were performed using the Winkler-type beam-on-spring model to evaluate the pipeline response in landslides. The FEA results showed that the stress and strain distribution along the pipeline were primarily positive, which indicated that the ground movement was resisted by axial tension force (membrane action) of the pipeline. The maximum axial strain occurred at the beginning and the end of the landslide zone, indicating that the pipeline would fail at these locations. The FEA results also indicated that the maximum axial forces in all cases were very close to the section capacity of the pipe, indicating that landslide-induced ground displacements resulted in very high axial force and relatively low bending moment in typical natural gas transmission pipelines. The PRCI guidelines provide an equation for estimating the anchor length of buried steel pipelines, but the results of this study indicate that the anchor lengths are much larger than those calculated by the PRCI equation. A proposed equation based on ultimate strength of the pipe section is suggested for calculating anchor length, which gives a good estimate of the anchor length with an average error of 4% relative to the analytical results. Overall, the study concluded that the internal pressure of the pipeline had no significant effect on the anchor lengths of the pipelines, and the proposed equation provides a more accurate estimate of the anchor length of typical natural gas transmission pipelines.

Keywords:
Landslide; Gas transmission pipeline; Anchor length; Finite element analysis

1. Introduction

Natural gas transmission pipelines are crucial components of the energy infrastructure, providing an essential source of fuel for homes, businesses and industries. However, these pipelines are vulnerable to various hazards along their route, such as landslides triggered by excessive rainfall or earthquakes. Landslides can disrupt the pipeline's integrity and cause significant damage, including leaks, ruptures and explosions.

Pipelines located in areas prone to landslides are at a higher risk of damage, which can result in economic and environmental losses. Disruptions caused by landslides have been shown to have direct and indirect economic consequences (Mori, et al., 2012). Large ground movements associated with landslides significantly deform the pipeline and result in excessive pipe stress. As the dimensions of the landslide increase, so does the force on the

pipeline, increasing the risk of damage (Zheng, et al., 2012). Studies indicate that landslides frequently contribute to gas pipeline failures globally. For example, between 2004 and 2013, about 85% of geotechnical-related failures and 11% of all natural-gas pipeline failures were caused by landslides (EGIG, 2015). Additionally, approximately 50% of pipeline ruptures in the Andes of South America have been attributed to landslides (Esford, et al., 2004).

Understanding the forces acting on a pipeline during a landslide is critical to comprehend its behavior. Figure (1) illustrates the forces acting on a pipeline due to landslide-induced ground displacement. At the boundaries of the landslide, shear forces occur on both sides of the moving soil mass, causing the pipeline to bend (IITK-GSDMA, 2007). Furthermore, friction between the soil and the pipeline creates an axial force within the pipeline, which varies depending on the diameter of the pipe, wall thickness and pipe material.

During a landslide, a significant length of a buried pipeline will move relative to the soil, activating friction between the soil and pipeline (PRCI, 2009). The point where the relative movement and friction fall to zero is known as the virtual anchor point. The distance between this point and the landslide where the relative movement occurs is called the anchor length. Figure (2) depicts the active length of a pipeline as the sum of the anchor lengths on each side of the landslide and the width of the landslide.

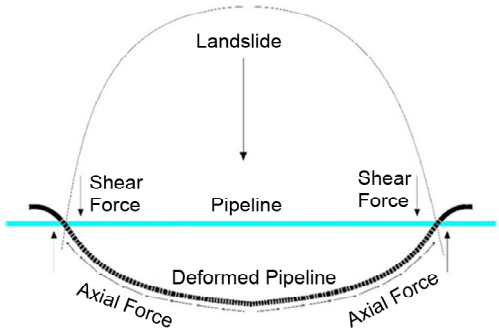

Figure 1. Forces acting on a pipeline during a landslide.

Accurate estimation of the active length is critical in the design process to reduce the risk of pipe damage. Studies have shown that the active length of a transmission pipeline is prone to damage during landslides; thus, this zone should be considered during the design and implementation of the pipeline. Installation of control and operating equipment, as well as bends, connections and joints in the pipe along the active length of the pipeline should be avoided in order to minimize the risk of pipeline failure.

In this study, Finite Element (FE) analyses were carried out to evaluate the response of typical natural gas transmission pipelines when they are subjected to landslide induced ground displacements. The goal of this research was to determine the length of pipe that will be affected by a landslide and provide a relationship for the anchor length based on nonlinear static finite element analyses. Nonlinear pipe elements were used to simulate the pipe, and nonlinear spring elements were employed to model the pipe-soil interaction. The investigation focused on typical pipelines with diameters of 12, 20, 30 and 48 inch under internal pressures of 0, 500 and 1000 psi buried at a depth of 1.20 m in either hard or soft soil.

2. Literature Review

Natural gas transmission pipelines play a crucial role in the energy infrastructure of many countries. However, the installation of these pipelines in mountainous regions can pose a risk due to landslides. Lee et al. (2016) discussed the issue of landslide risks associated with pipelines in

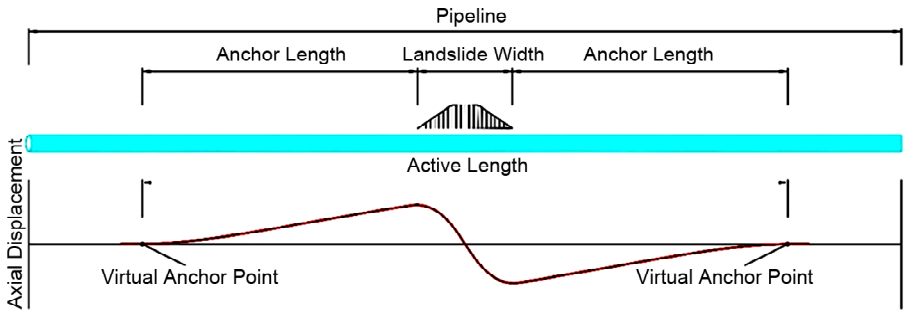

Figure 2. Active length and anchor length of pipeline.

mountainous terrain. The authors investigated several case studies and provided recommendations to mitigate potential hazards. They highlighted the importance of proper site investigation, design considerations, and construction techniques to reduce the risks associated with pipeline installation in such regions.

Kennedy et al. (1977) conducted an experimental study to determine the effects of fault movements on buried oil pipelines. The study aimed to investigate the behavior of the pipeline and its response to fault movements. The authors concluded that pipeline deflection during fault movement depends on various factors such as the pipeline material properties, soil strength, and burial depth.

Wang and Yeh (1985) presented a refined seismic analysis of buried pipelines for fault movement. The authors developed a finite element model to analyze the behavior of pipelines subjected to seismic loads due to fault movement. The study highlighted the importance of considering the effect of soil-pipe interaction on pipeline behavior.

Chiou et al. (1994) studied the response of buried pipelines to fault movements using finite element analysis. The authors considered various parameters such as pipe diameter, burial depth, and fault displacement. The study showed that the maximum strain in pipelines significantly increases with increasing fault displacement and decreasing burial depth.

Liu and O'Rourke (1997) investigated the behavior of continuous pipelines subjected to transverse permanent ground deformation (PGD) during earthquakes. The authors analyzed the effect of PGD on pipeline behavior and proposed a simplified design method for buried pipelines subjected to this type of loading.

O'Rourke and Liu (2012) presented a comprehensive review of the seismic design of buried and offshore pipelines. The authors discussed various design aspects such as seismicity, soil-structure interaction, and pipeline material properties. They also provided recommendations for designing pipelines that can withstand seismic loads.

Banushi and Squeglia (2018) developed equivalent-boundary conditions for seismic analysis of buried operating steel pipelines. The authors used the finite element method to simulate the behavior of pipelines subjected to seismic loads. The study showed that the proposed methodology can provide accurate results while reducing computational effort and time.

Vasseghi et al. (2021) carried out a failure analysis of a natural gas pipeline subjected to a landslide. The authors used numerical simulation to investigate the behavior of the pipeline and identified the causes of failure. The study highlighted the importance of considering the effects of soil strength, pipeline material properties, and pipeline geometry on the behavior of pipelines during landslides. This study also indicated that the anchor length calculated by the PRCI equation underestimates the actual anchor length.

Demirci et al. (2021) conducted experimental and numerical studies to analyze the behavior of buried continuous pipelines crossing strike-slip faults. The authors investigated the effect of fault width, burial depth, and pipeline diameter on pipeline behavior. The study showed that the pipeline's maximum stress significantly increases with increasing fault width and decreasing burial depth.

Overall, the reviewed papers provide valuable insights into the behavior of buried pipelines under permanent ground displacements. The studies highlight the importance of considering various factors such as soil-pipeline interaction, pipeline material properties, and pipeline geometry when designing pipelines in mountainous regions. The literature suggests that the anchor length of pipelines subject to landslides is influenced by a variety of factors including slope inclination, soil properties, pipeline burial depth, and pipe properties. These findings can help improve the design practices and mitigate the risks associated with pipeline installation in such areas. However, further research is needed to fully understand the complex interactions between these factors and to develop more effective strategies for ensuring the safety and reliability of natural gas transmission pipelines in landslide-prone areas.

3. Numerical Modeling

The present study utilized ANSYS finite element software to evaluate the behavior of typical pipelines during landslides. The pipeline

orientations were assumed to be perpendicular to the direction of landslide movement. Nonlinear static analysis was performed on FE models of the pipelines under various conditions. The FE models consisted of pipe elements supported by Winkler-type springs, where the soil-pipe interaction was modeled using nonlinear spring elements. Nonlinear two-node pipe elements are used to represent the pipeline. The pipe element (PIPE-288) has the capability to simulate large plastic strain, but it could not simulate local bucking failure. However, pipelines oriented perpendicular to the direction of landslide movement are not susceptible to local buckling failure. They resist the landslide movement by developing axial tension in the pipe, and the failure mode is typically ruptured due to the high axial tension (PRCI, 2009; Vasseghi et al., 2021).

The FE model had a total length of 1500 m and included 500 pipe elements (3 m long) with three discrete spring elements at each node. It was assumed that the pipe element was thick-walled with a linear shape function. The analyses were conducted in two stages, where internal pressure was applied to the pipe elements during the first stage, and landslide-induced ground displacement was applied to the base of the corresponding soil springs in the second stage. The pipeline response was evaluated at internal pressures of zero, 3.45 MPa (500 psi), and 6.90 MPa (1000 psi).

3.1. Landslide Displacement

The ground movement was simulated by applying displacement compatible with that of a landslide to the ground end of the spring elements. Different functions were considered to describe the landslide displacement pattern. O'Rourke (1988) suggested a beta probability density function to approximate the landslide displacement profile. O'Rourke (1989) used a simple cosine function and Suzuki et al. (1988) proposed a cosine function raised to the power of n to define the displacement pattern of landslides as:

$$y(x)=\delta\left[1-\left(\cos\frac{\pi x}{W_s}\right)^n\right] \quad (1)$$

where $y(x)$ is the ground displacement across the landslide, x is the distance measured from the center of the landslide, δ is the peak ground displacement, W_S is the landslide width and n is an even integer number. This equation that is also recommended by the Pipeline Research Council International (PRCI, 2009) was used for this study. The profile for a landslide width of WS = 120 m, peak ground displacement of $\delta = 20$ m, and $n = 10$ is shown in Figure (3).

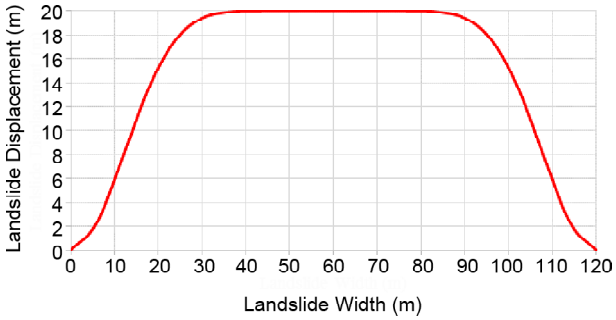

Figure 3. Ground displacement pattern.

3.2. Soil and Pipe Material Properties

Pipelines with diameters of 12, 20, 30 and 48 inches at a burial depth of 1.20 m were analyzed in this study. In the guidelines of the Seismic Design of Buried Pipelines (IITK-GSDMA, 2007), it is recommended that the backfill soil around the pipeline should be loose granular soil to reduce the forces on the pipeline. In this study, conventional loose sand was considered as the backfill soil around the pipe. The trench was assumed to be filled initially by loose sand and then by native soil as shown in Figure (4). The native soil was assumed to be either soft soil (loose clay) or hard

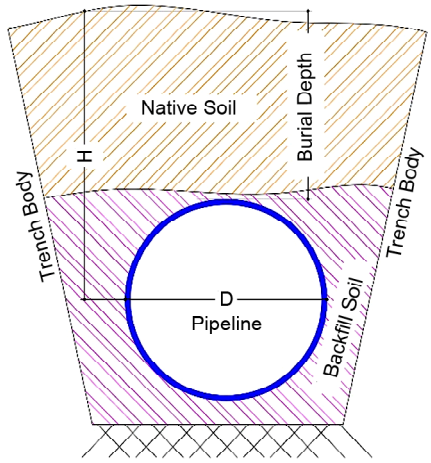

Figure 4. Trench backfill.

soil (dense sand). The characteristics of these soils and the loose sand are tabulated in Table (1), where γ is the density, ϕ is the internal friction angle and *c* is the cohesion factor of the soil.

Table 1. Soil properties.

Soil	γ (kN/m³)	ϕ (Degree)	*c* (kN/m²)
Soft Clay (Soft)	16.5	---	40
Dense Sand (Hard)	19.5	40	---
Loose Sand (Backfill)	16.5	35	---

The pipes are made of API-5L steel, which has a modulus of elasticity of 2.1×105 MPa and a Poisson's ratio of 0.3. The X42 steel grade is used for the 12 and 20 inch pipes, while the 30 and 48 inch pipes use X52 and X65 respectively. To account for variability in strength, expected yield strength (F_{ye}) and expected ultimate strength (F_{ue}) are assumed to be 20% greater than the nominal strength. Table (2) provides details on the diameters, wall thicknesses, and nominal and expected strengths for each pipe.

According to ATC/DOT/99 (Haggag, 1999), the nonlinear behavior of steel pipes material can be described by the stress-strain relationship, expressed as:

$$\sigma_t = K \varepsilon_p^m \tag{2}$$

where σ_t is the stress, ε_p is the plastic strain, *K* is the strength coefficient and *m* is the strain hardening exponent. Table (3) shows the recommended values for coefficients K and m for each steel grade. Figure (5) shows the stress-strain curves of the X42, X52, and X65 steel based on Equation (2) and the fitted multi-linear curve considered for analysis.

3.3. Soil-Pipe Interaction

The soil-pipe interaction was modeled using Winkler theory, which utilized springs in the axial, vertical, and lateral directions to represent the soil's behavior surrounding the pipe. The load-deformation curve of each spring is represented in Figure (6), and the parameters for these idealized curves are dependent on both the soil and pipe properties, as described in the ALA guidelines (ASCE, 1984).

In accordance with the ALA guidelines for the design of buried steel pipes (ASCE, 1984), the axial soil spring force was calculated based on the backfill soil (loose sand), and the other soil spring forces were calculated based on the native soil properties. The axial soil resistance (T_u) per unit length of the pipeline for the steel pipe laid in the loose sand can be calculated as:

$$T_u = \pi D\, \alpha c + \pi D\, H \gamma \left(\frac{1 + \frac{K_0}{2}}{2} \right) tan\, \delta \tag{3}$$

where *D* is the pipe diameter, α is the adhesion factor, *c* is the soil cohesion, *H* is the depth of cover to the pipe centerline, γ is the unit weight

Table 2. Pipe dimensions and material properties.

Case	Diameter	Thickness (mm)	Grade	Nominal Strength (MPa)		Expected Strength (MPa)	
				Yield Strength (F_y)	Ultimate Strength (F_u)	Yield Strength (F_{ye})	Ultimate Strength (F_{ue})
1	12 in	6	X42	290	441	348	497
4	20 in	7.5	X42	290	414	348	497
7	30 in	9	X52	359	462	431	554
10	48 in	12	X65	448	531	538	637

Table 3. K and m coefficients for steel pipes.

Grade	Strength Coefficient (K) (MPa)	Strain Hardening Exponent (*m*)
X42	648.0	0.099
X52	685.0	0.076
X65	770.4	0.059
X75	832.5	0.064

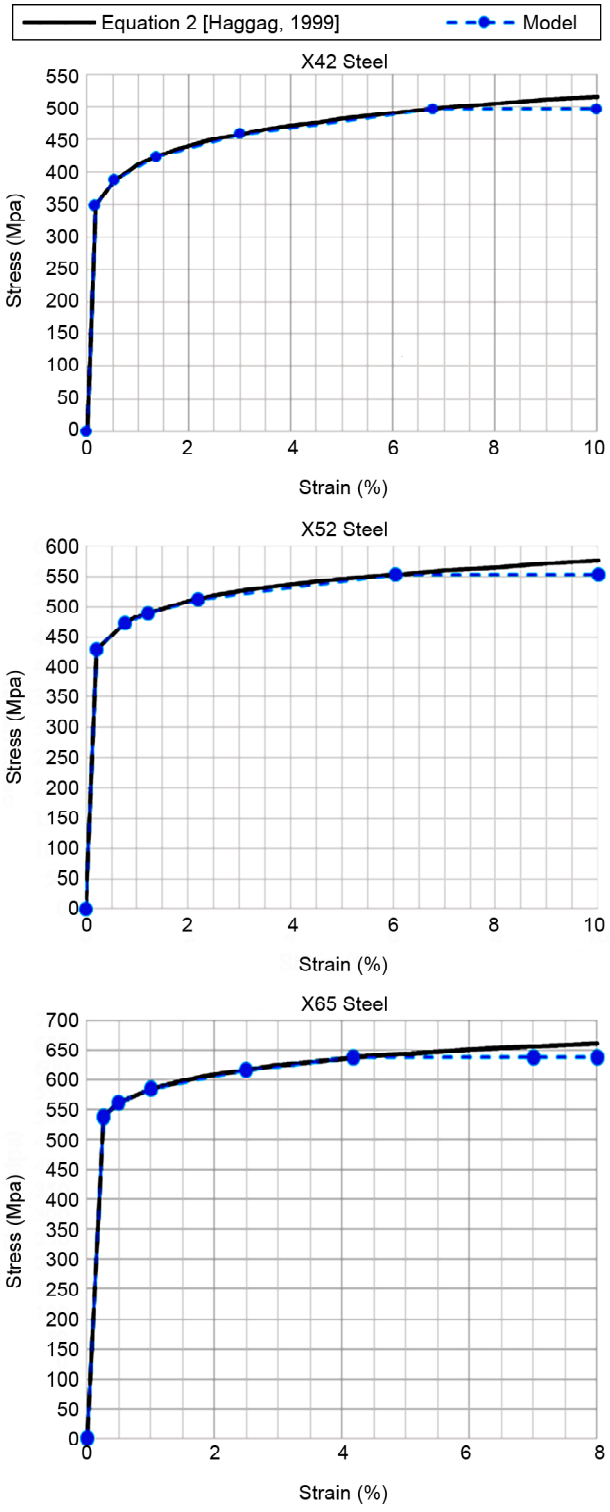

Figure 5. Stress-strain curves for API-grade steel pipes.

of the soil, K_0 is the coefficient of pressure at rest and δ is the angle of internal friction at the soil-pipe interface. According to the guideline for the seismic design of oil and gas pipeline systems (ASCE, 1984), the recommended values for K_0 and δ are 0.37 and 31, respectively. These values comply with the pull-out tests of an 18-in steel pipe embedded in loose sand (Wijewickreme, et al., 2009). The equation for calculating the maximum lateral soil resistance of a buried pipeline is:

$$P_u = N_{ch} cD + N_{qh} \gamma HD \tag{4}$$

where N_{ch}, and N_{qh} are the horizontal bearing factors for clay and sand, respectively. The equation for calculation of the maximum vertical bearing soil resistance per unit length of the pipeline is:

$$Q_d = N_c cD + N_q \gamma HD + N_\gamma \gamma \frac{D^2}{2} \tag{5}$$

where N_c, N_q, and N_γ, are the vertical bearing capacity factors. The equation for calculation of the maximum vertical uplift soil resistance per unit length of the pipeline is:

$$Q_u = N_{cv} cD + N_{qv} \gamma HD \tag{6}$$

where N_{cv} and N_{qv} are the vertical uplift factor for clay and sand, respectively. The ALA guidelines (Alliance, 2001) provide closed-form expressions for evaluating vertical uplift, vertical bearing, and horizontal bearing factors. Table (4) lists the computed elastic properties of the Winkler springs as derived from Equation (3) through Equation (6). The soil spring forces were calculated for a 3-m long pipe to match the element size in the FEA model. The yield displacement for each spring was calculated according to ALA guidelines.

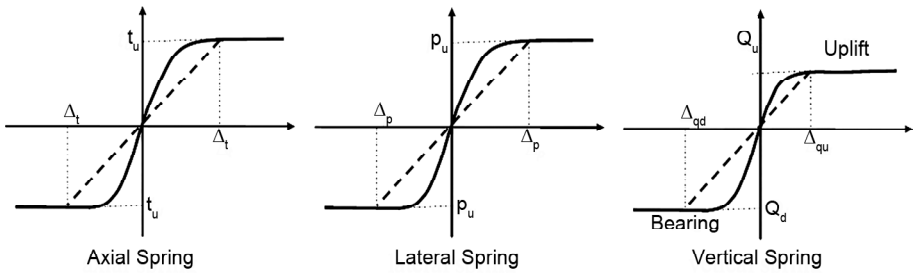

Figure 6. Idealized load-deformation curves for soil springs (ASCE, 1984).

Table 4. Soil spring properties.

Spring	Soil	Force (kN)	Displacement (mm)	Force (kN)	Displacement (mm)	Force (kN)	Displ. (mm)	Force (kN)	Displacement (mm)
		12 inch		20 inch		30 inch		48 inch	
Longitude.	Soft	$T_u = 26.4$	$\Delta_t = 5$	$T_u = 47.3$	$\Delta_t = 5$	$T_u = 77.1$	$\Delta_t = 5$	$T_u = 141.2$	$\Delta_t = 5$
Lateral		$P_u = 245.4$	$\Delta_p = 46$	$P_u = 385.3$	$\Delta_p = 68$	$P_u = 545.2$	$\Delta_p = 78$	$P_u = 807.6$	$\Delta_p = 97$
Vertical Uplift		$Q_u = 324.6$	$\Delta_{qu} = 61$	$Q_u = 349$	$\Delta_{qu} = 102$	$Q_u = 379.4$	$\Delta_{qu} = 152$	$Q_u = 434.3$	$\Delta_{qu} = 181$
Vertical Bearing		$Q_d = 208.7$	$\Delta_{qd} = 61$	$Q_d = 350.5$	$\Delta_{qd} = 102$	$Q_d = 531$	$\Delta_{qd} = 152$	$Q_d = 864.5$	$\Delta_{qd} = 244$
Longitude.	Hard	$T_u = 31.2$	$\Delta_t = 5$	$T_u = 55.9$	$\Delta_t = 5$	$T_u = 91.1$	$\Delta_t = 5$	$T_u = 166.9$	$\Delta_t = 5$
Lateral		$P_u = 463.9$	$\Delta_p = 46$	$P_u = 704.2$	$\Delta_p = 68$	$P_u = 1043.1$	$\Delta_p = 78$	$P_u = 1766.4$	$\Delta_p = 97$
Vertical Uplift		$Q_u = 97.3$	$\Delta_{qu} = 14$	$Q_u = 112.1$	$\Delta_{qu} = 15$	$Q_u = 132.9$	$\Delta_{qu} = 16$	$Q_u = 174.1$	$\Delta_{qu} = 18$
Vertical Bearing		$Q_d = 1864.8$	$\Delta_{qd} = 30$	$Q_d = 3603.8$	$\Delta_{qd} = 51$	$Q_d = 6391.6$	$\Delta_{qd} = 76$	$Q_d = 13065.8$	$\Delta_{qd} = 122$

3.4. Verification of FE Model

The FE model was verified by comparing its results with those of a failure analysis conducted by (Vasseghi, et al., 2021) on a 16-inch pressurized natural gas pipeline that experienced the Taleghan landslide. The comparison is shown in Figure (7), which illustrates the maximum lateral and vertical displacements induced by the landslide in both models.

Vasseghi et al. (2021) reported maximum displacements of 5.86 m and 3.99 m for lateral and vertical directions, respectively. In the current model, the lateral displacement was 5.80 m and the vertical displacement was 3.93 m, indicating good agreement between the two models. Moreover, the vertical and lateral displacement patterns of the pipeline were nearly identical in both models. The stress intensity, longitudinal strain, axial force, and bending moment results from the current study were also in good agreement with those reported by Vasseghi et al. (2021).

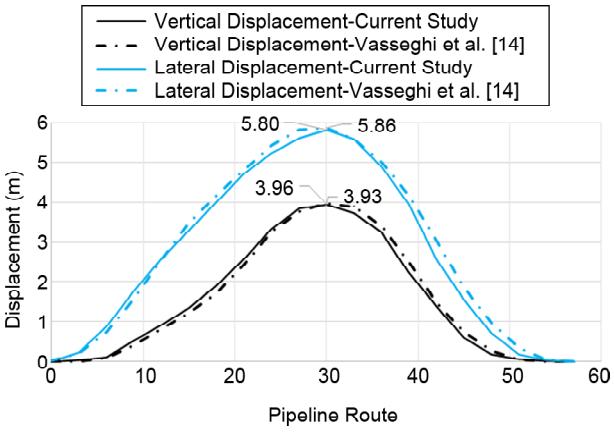

Figure 7. Pipeline displacements from current study and (Vasseghi, et al., 2021).

4. FEA Results

To evaluate the active lengths of pipelines in landslides, it is necessary to define a failure criterion for the pipe. The failure mode of a pipeline oriented perpendicular to the direction of the landslide movement is pipe rupture due to excessive tensile strain (Vasseghi, et al., 2021). The ultimate strain of API-grade steel pipes is typically more than 20%. However, according to a comprehensive study on pipeline failures (Kunert, et al., 2016), rupture failure of pipelines due to ground movement occurs almost always at the girt welds or heat affected zone (HAZ) of the welds. Therefore, the design guidelines define failure criteria based on the strain capacity of the welds, which is much lower than the ultimate strain of the pipe material. The limiting tensile strain in the ALA guidelines is 2% for the operational limit state and 4% for the pressure integrity limit state (Alliance, 2001). In this study, it is assumed that the pipe would rupture at an axial tension strain of 5%, and this strain is used as the failure criterion for the pipe.

The FE model of each pipeline was subjected to the ground displacement pattern shown in Figure (3) up to a displacement that would result in pipeline failure (i.e., a maximum axial tension strain of 5%). The analyses were conducted for pipe internal pressures of zero, 500 psi, and 1000 psi. The maximum landslide displacements associated with pipe tension strain of 5% are listed in Table (5). The landslide displacements at the limit state (5% tension strain) in hard soils are significantly less than those in soft soil. These displacements are only marginally affected by the

Table 5. Landslide displacements associated with pipe tensile strain of 5%.

Pipe Dia. (in)	Hard Soil			Soft Soil		
	P = 0	P = 500 psi	P = 1000 psi	P = 0	P = 500 psi	P = 1000 psi
12	9.32	9.43	9.50	10.05	10.09	10.25
20	10.11	10.12	10.33	12.57	12.65	12.85
30	11.90	12.00	12.24	14.61	14.78	14.83
48	12.99	13.35	13.39	18.61	18.61	18.72

internal pressure.

The FEA results are evaluated at the limit state of 5% tension strain. Figure (8) shows the results of the axial strain along the 30-in pipeline at 500 psi for both soft and hard soils. As shown, the limit state in the pipeline (i.e., 5% axial strain) occurred at the beginning and the end of the landslide zone, indicating that the pipeline would fail at these locations.

Figure (9) shows the stress intensities at the limit state for the 30-in pipeline. As shown, a relatively large length of the pipeline was yielded. The pipe stress near the boundaries was caused by bending deformation and membrane action of the pipeline. The pipeline outside the landslide zone was mainly subjected to axial tensile stress caused by the membrane action.

At zero and 1000 psi internal pressures, the axial strain and stress intensity of the pipeline were similar to those at 500 psi pressure. Figures (8) and (9) indicate that at the limit state, the stress and strain distribution along the pipeline are essentially positive. This is an indication that the ground movement is primarily resisted by axial tension

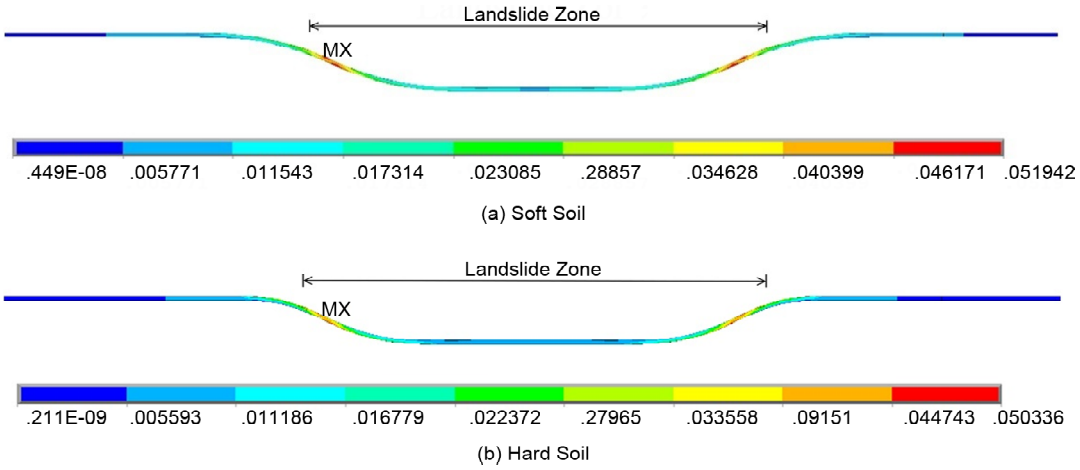

Figure 8. Longitudinal strain distribution over 30-in pipe, at 500 psi

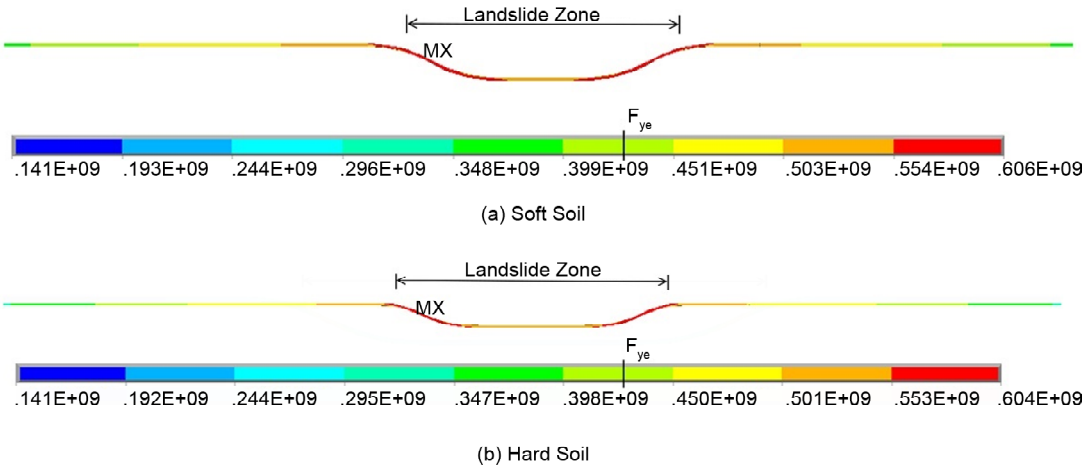

Figure 9. Stress intensity distribution of a 30-in pipe at 500 psi.

force (membrane action) of the pipeline.

Figure (10) shows typical distributions of pipe axial displacement and the pipe-soil frictional force (axial soil spring force) at the limit state. This figure indicates that the anchor length of the pipeline where the friction at the pipe-soil interface is activated extends well beyond the landslide zone. Along this length that is much larger than the landslide width, the axial soil springs reach their maximum capacity. The fluctuation of the axial soil spring forces within the landslide zone is mainly due to yielding of the pipeline in this area.

4.1. Axial force and Bending Moment of Pipeline

The axial force and bending moment distribution in the pipeline demonstrate the behavior of the pipeline during landslide. Figure (11) shows the distributions of the axial force along the pipelines at 500 psi internal pressure. This force has been normalized as:

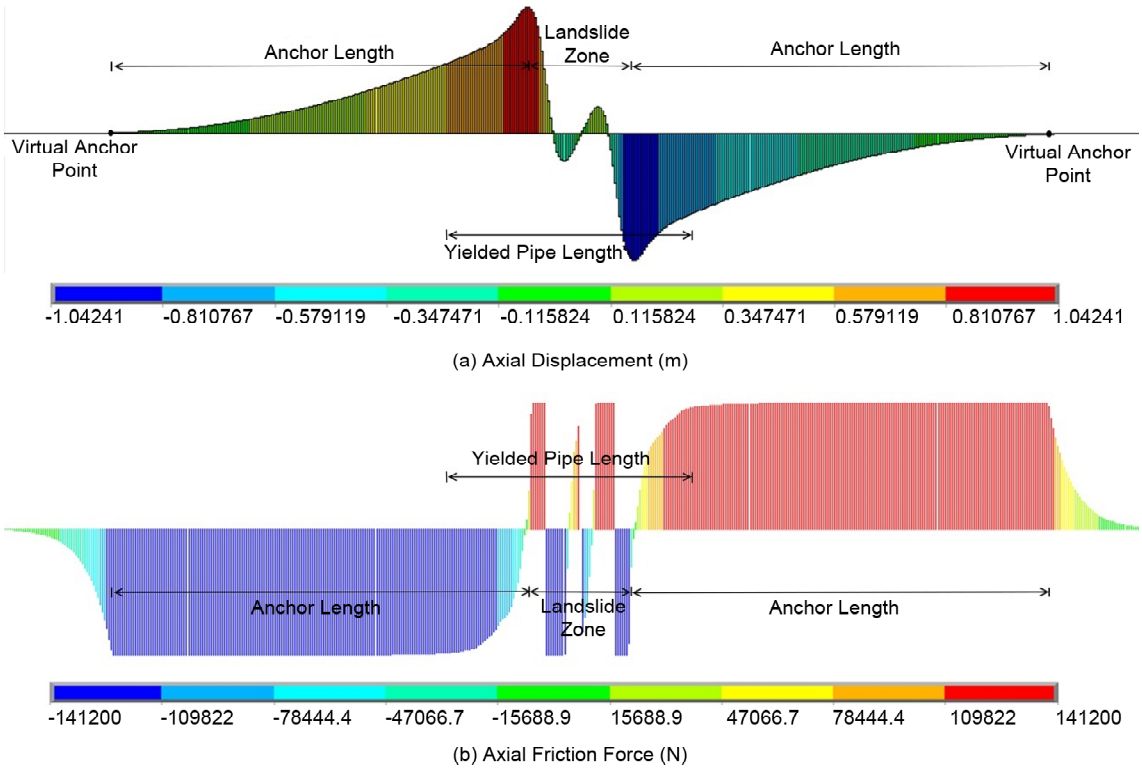

Figure 10. Typical distributions of pipe axial displacement and friction at pipe-soil interface.

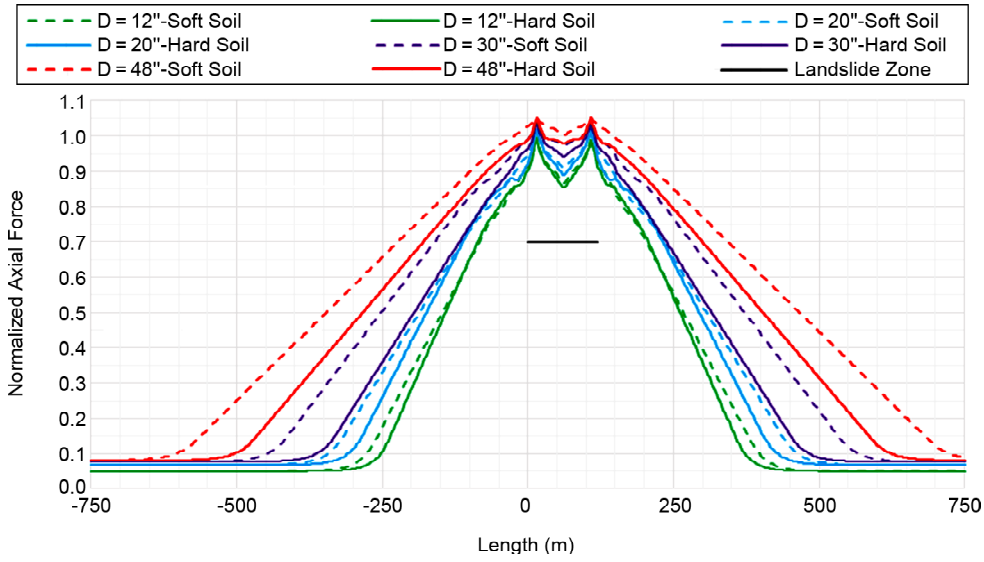

Figure 11. Axial force distribution along pipeline subjected to landslide at 500 psi pressure.

$$F_{norm} = \frac{F}{A \times F_{ue}} \tag{8}$$

where F is the pipe axial force at the limit state, A is the pipe cross-sectional area and F_{ue} is the expected ultimate stress of the pipe material.

Figure (11) indicates that the axial force distributions are similar for all analyses, with maximum axial force occurring near the boundary of the landslide zone. However, the extent of axial force distribution along the pipeline increases with increasing pipe diameter. The axial force distributions also extend farther in the soft soil relative to the hard soil. This figure also indicates that the maximum axial forces in all the cases are very close to the section capacity of the pipe. Figure (12) shows the effect of internal pressure on the maximum axial forces in the pipelines. As shown, the axial force marginally increases with increasing internal pressure. This increase is due to increased axial capacity of the pipe when it is subjected to high internal pressure.

Figure (13) shows the distribution of the bending moment along the pipeline at 500 psi internal pressure. For purposes of comparison, the bending moment has been normalized as:

$$M_{norm} = \frac{M}{Z \times F_{ue}} \tag{9}$$

$$Z = \frac{1}{6}\left(D_o^3 - D_i^3\right) \tag{10}$$

where M is the pipe bending moment at the limit state, Z is the plastic section modulus of the pipe, D_o is the outer diameter of the pipe, and D_i is the inner diameter of the pipe.

Figure (13) indicates that the bending moment distributions only extend a short distance (less

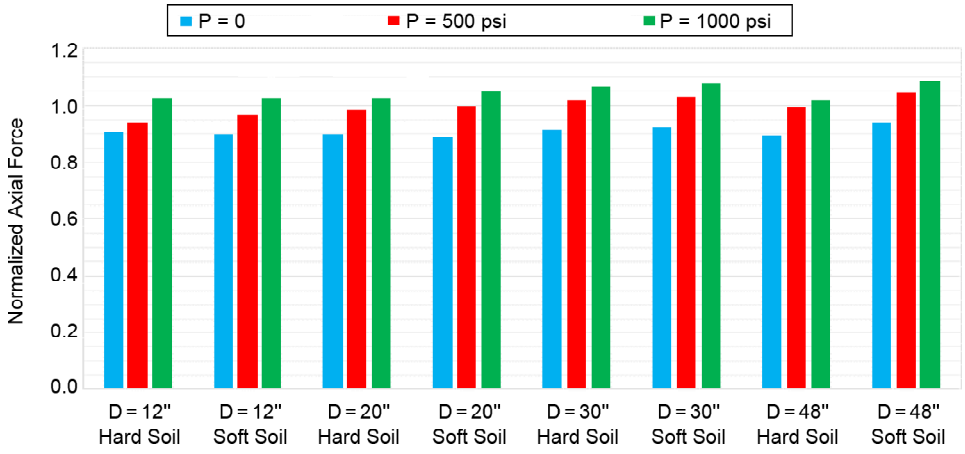

Figure 12. Normalized maximum axial force of pipelines with different internal pressures.

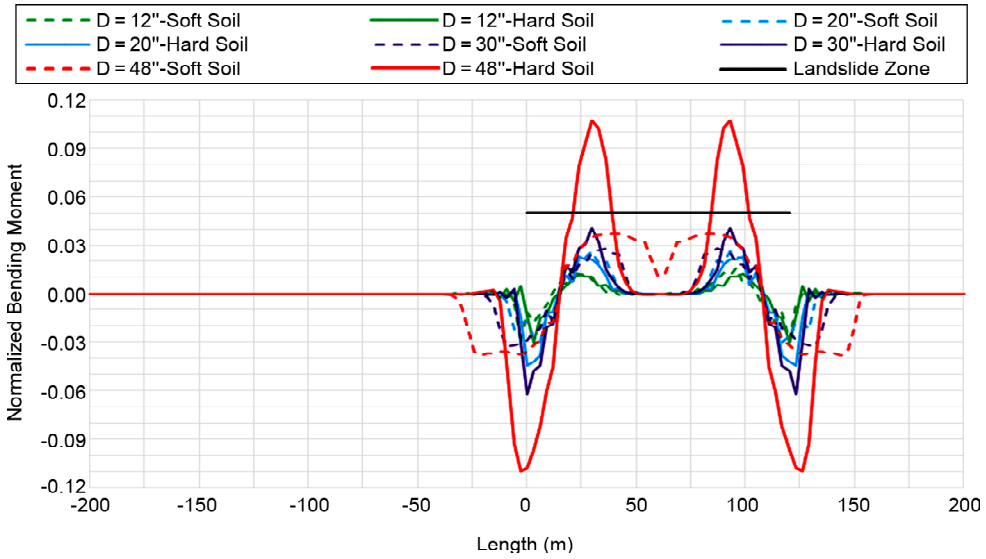

Figure 13. Bending moment distribution along pipeline subjected to landslide at 500 psi pressure.

than 30 m) beyond the landslide boundaries. This extension decreases with increasing soil hardness. The maximum bending generally occurs near the landslide boundaries and it increases with increasing pipe diameter. This figure also indicates that the 48 inch pipeline in hard soil experiences the highest bending moment at 10.6% of the section capacity. For the 48 inch pipeline in soft soil, the maximum bending is reduced to 3.8% of the section capacity. Figure (14) shows the effect of internal pressure on the maximum bending moment. Again, the bending moment only marginally increases with increasing internal pressure.

Figures (11) to (14) indicate landslide induced ground displacements result in very high axial force and relatively low bending moment in typical natural gas transmission pipelines. As a result, the anchor length is highly affected by the axial capacity of the pipe.

4.2. Anchor Length of Pipeline

The PRCI guideline (PRCI, 2009) provides the following equation for estimating the anchor length of buried steel pipelines.

$$L_a = \frac{\pi D t F_y}{T_u} \tag{11}$$

where D is the pipe diameter, t is the wall thickness, F_y the yield stress of the pipe material, and T_u is the maximum friction force at the pipe-soil interface calculated as per Equation (3). The anchor length derived from the analyses is the clear distance between the landslide and the virtual anchor point, where the axial displacement of the pipeline diminishes to zero. The axial displacements of the pipelines with 500 psi internal pressure are shown in Figure (15). The results of the analyses indicate that the anchor lengths are much larger those calculated by Equation (7). Figure (16) compares the anchor lengths derived from the analyses with the anchor length calculated by the PRCI equation. This figure indicates that the anchor lengths are not significantly affected by internal pressure, but they are substantially larger than the PRCI calculated length. In general, the anchor length calculated by the PRCI equation is, on average, 35% less than the analytical anchor length. Due to the high pipe tension, the installation of valves, bends, and other accessories is usually avoided along the anchor length in order to reduce the risk of failure of pipelines crossing a potential landslide. Thus, the PRCI equation is unconservative and can lead to pipe failure if such items are installed along the anchor length.

4.3. Proposed Equation for Anchor Length

The results of the analyses indicate that the pipeline stress intensity exceeded the ultimate stress (F_u) at the limit state. This indicates that replacing the yield strength (F_y) with the ultimate strength (F_u) will improve the PRCI equation. A coefficient which collectively accounts for the internal pressure, ratio of expected to nominal strength, effect of bending moment, and soil type

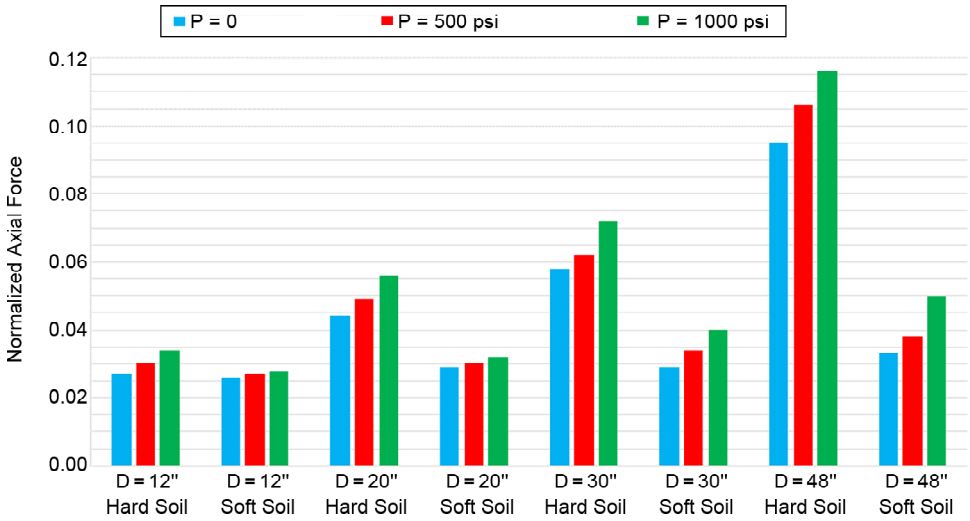

Figure 14. Normalized maximum bending moment of pipeline with different internal pressures.

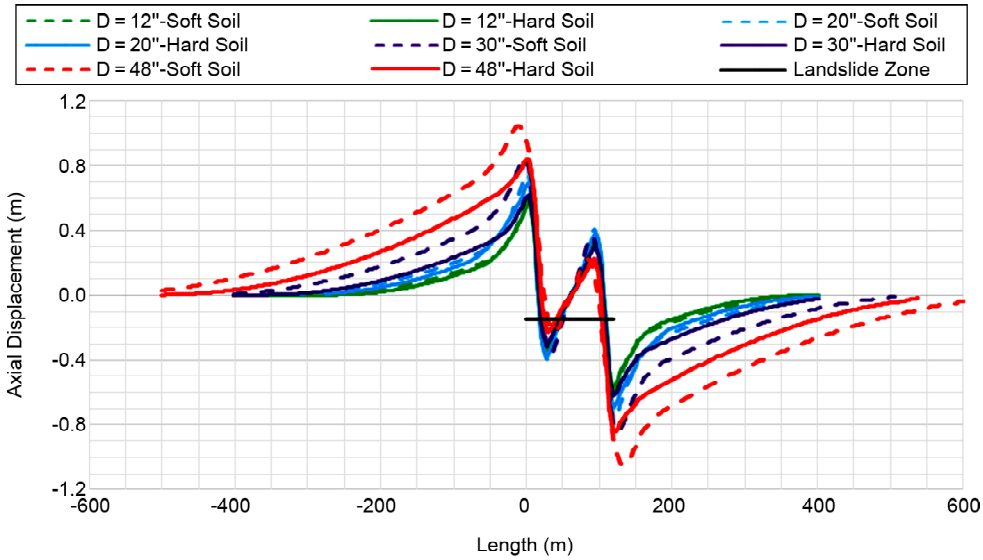

Figure 15. Axial displacement of pipeline subjected to landslide at 500 psi for different cases.

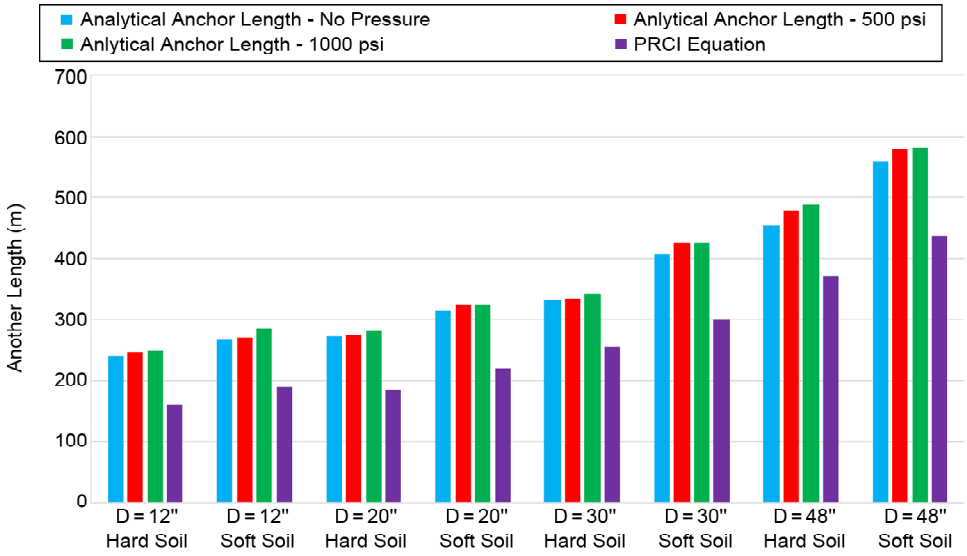

Figure 16. Comparison of anchor length calculated by PRCI equation with analysis results.

needs to be included in the equation. Upon reviewing the analytical data, the following equation is proposed for estimating the anchor length of typical natural gas transmission pipelines.

$$L_{a-proposed} = 1.1 \times \frac{\pi D t F_u}{T_u} \tag{12}$$

Table (6) compares the anchor lengths calculated by Equation (12) with the analysis results and lists the corresponding errors which are less than 10%. The negative sign in the error indicates that the anchor length estimated from the proposed equation is greater than the analytical results. The average error is 4% and thus Equation (12) gives a good estimate of the anchor length. The comparison of the anchor lengths is shown in Figure (17).

5. Conclusion

In this study, finite element analyses were performed to evaluate the behavior of typical natural gas transmission pipelines in landslides and investigate the effect of various parameters on their anchor lengths. The main conclusions drawn from the results of this study are:

- Landslide-induced ground displacements result in very high axial force and relatively low bending moment in typical natural gas transmission pipelines.
- The ground displacement is primarily resisted by the membrane action of the pipeline.

Table 6. Total error in anchor length calculated using Equation (12) and analytical anchor length.

Dia. (in)	Soil	Internal Pressure (psi)	Analytical Anchor Length (m)	Proposed Anchor Length (m)	Total Error (%)
12	Hard	0	239	252	-5.44
12	Hard	500	246	252	-2.44
12	Hard	1000	248	252	-1.61
20	Hard	0	273	292	-6.96
20	Hard	500	275	292	-6.18
20	Hard	1000	282	292	-3.55
30	Hard	0	331	360	-7.68
30	Hard	500	333	360	-8.11
30	Hard	1000	342	360	-5.26
48	Hard	0	454	482	-6.17
48	Hard	500	479	482	-0.63
48	Hard	1000	486	482	-0.82
12	Soft	0	269	297	-10.04
12	Soft	500	270	297	-10.00
12	Soft	1000	286	297	-3.85
20	Soft	0	315	346	-9.84
20	Soft	500	324	346	-6.79
20	Soft	1000	325	346	-6.46
30	Soft	0	408	425	-4.17
30	Soft	500	425	425	0.00
30	Soft	1000	426	425	0.23
48	Soft	0	559	570	-1.97
48	Soft	500	578	570	1.38
48	Soft	1000	580	570	1.72

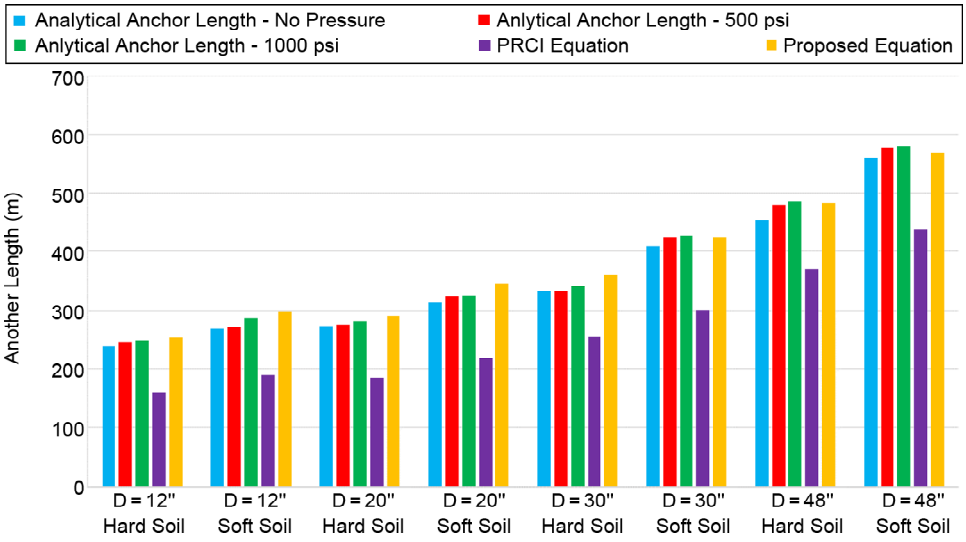

Figure 17. Anchor length calculated using Equation (11) and analysis results.

- The internal pressure of the pipeline has no significant effect on the anchor lengths of the pipelines.
- The equation in the PRCI guidelines, which is based on nominal yield strength of the pipe section, significantly underestimates anchor length.
- An equation which is based on ultimate strength of pipe section is proposed for the anchor length.
- The proposed equation provides a reliable estimate of anchor length with an average error of only 4% when compared to analytical results.

Acknowledgments

The research project (Project No. 768) leading to this paper was sponsored by the International Institute of Earthquake Engineering and Seismology (IIEES).

References

Alliance, A.L. (2001). *Guidelines for the Design of Buried Steel Pipe*. American Society of Civil Engineers.

ASCE. (1984). *Guidelines for the Seismic Design of Oil and Gas Pipeline Systems*. American Society of Civil Engineers.

Banushi, G., & Squeglia, N. (2018). Seismic analysis of a buried operating steel pipeline with emphasis on the equivalent-boundary conditions. *Journal of Pipeline Systems Engineering and Practice*, *9*(3).

Chiou, Y., Chi, S., & Chang, H. (1994). A study of buried pipeline response to fault movement. *Journal of Pressure Vessel Technology*, *116*(1).

Demirci, H.E., Karaman, M., & Bhattacharya, S. (2021). Behaviour of buried continuous pipelines crossing strike-slip faults: Experimental and numerical study. *Journal of Natural Gas Science and Engineering*, *92*.

EGIG. (2015). *Gas Pipeline Incidents: 9th Report of the European Gas Pipeline Incident Data Group (period 1970 - 2013). Doc. Number EGIG 14.R.0403*. Groningen, the Netherlands: European Gas Pipeline Incident Data Group.

Esford, F., Porter, M., Savigny, K.W., Muhlbauer, W., & Dunlop, C. (2004). A risk assessment model for pipelines exposed to geohazards. *International Pipeline Conference*, 2557-2565.

Haggag, F. (1999). *Nondestructive Determination of Yield Strength and Stress-Strain Curves of In-Service Transmission Pipelines Using Innovative Stress-Strain MicroprobeTM Technology*. Washington, DC.: Advanced Technology Corporation.

IITK-GSDMA. (2007). *Guidelines for Seismic Design of Buried Pipelines*. Indian Institute of Technology Kanpur (IITK) and Gujarat State Disaster Management Authority (GSDMA).

Kennedy, R., Williamson, R., & Chow, A. (1977). Fault movement effects on buried oil pipeline. *Transportation Engineering*, *103*(5), 617-633.

Kunert, H.G., Marquez, A.A., Fazzini, P., & Otegui, J.L. (2016). Failures and integrity of pipelines subjected to soil movements. *In Handbook of Materials Failure Analysis with Case Studies from the Oil and Gas Industry*, 105-122. Butterworth-Heinemann.

Lee, E., Fookes, P., & Hart, A. (2016). Landslide issues associated with oil and gas pipelines in mountainous terrain. *Quarterly Journal of Engineering Geology and Hydrogeology*, *49*(2), 125-131.

Liu, X., & O'Rourke, M. (1997). Behaviour of continuous pipeline subject to transverse PGD. *Earthquake Engineering & Structural Dynamics*, *26*(10), 989-1003.

Mori, S., Chiba, K., & Koike, T. (2012). Seismic performance analysis of the transmission Gas pipeline in the 2011 Great East Japan earthquake. *15th World Conference on Earthquake Engineering* (15WCEE), 24-28.

O'Rourke, M. (1989). Approximate analysis procedures for permanent ground deformation effects on buried pipelines. *The Second US Japan Workshop on Liquefaction, Large Ground Deformation and Their Effects on Lifelines*, 336-347. Buffalo, New York: Multidisciplinary Center for Earthquake Engineering Research.

O'Rourke, M., & Liu, X. (2012). *Seismic Design of Buried and Offshore Pipelines (MCEER-12-MN04). MCEER*.

O'Rourke, T. (1988). Critical aspects of soil-pipeline interaction for large ground deformation. *1st Japan-US Workshop on Liquefaction, Large Ground Deformation and Their Effects on Lifelines*, 118-126. Japan: Association for Development of Earthquake Prediction.

PRCI. (2009). *Pipeline Integrity for Ground Movement Hazards*. Houston: Pipeline Research Council International.

Suzuki, N., Arata, O., & Suzuki, I. (1988). Subject to liquefaction-induced permanent ground displacement. *The First Japan-US Workshop on Liquefaction, Large Ground Deformation and their Effects on Lifeline Facilities*. Tokyo, Japan.

Vasseghi, A., Haghshenas, E., Soroushian, A., & Rakhshandeh, M. (2021). Failure analysis of a natural gas pipeline subjected to landslide. *Engineering Failure Analysis*, *119*.

Wang, L., & Yeh, Y. (1985). A refined seismic analysis and design of buried pipeline for fault movement. *Earthquake Engineering & Structural Dynamics*, *13*(1), 75-96.

Wijewickreme, D., Karimian, H., & Honegger, D. (2009). Response of buried steel pipelines subjected to relative axial soil movement. *Canadian Geotechnical Journal*, *46*(7), 735-752.

Zheng, J., Zhang, B., Liu, P., & Wu, L. (2012). Failure analysis and safety evaluation of buried pipeline due to deflection of landslide process. *Engineering Failure Analysis*, *25*, 156-168.